



Universidad Autónoma  
de Madrid

**Biblos-e Archivo**  
Repositorio Institucional UAM

**Repositorio Institucional de la Universidad Autónoma de Madrid**  
<https://repositorio.uam.es>

Esta es la **versión de autor** del artículo publicado en:  
This is an **author produced version** of a paper published in:

Waste Management 105 (2020): 566-574

**DOI:** <https://doi.org/10.1016/j.wasman.2020.03.004>

**Copyright:** © 2020 Elsevier Ltd.

El acceso a la versión del editor puede requerir la suscripción del recurso  
Access to the published version may require subscription

# Energy and phosphorous recovery through hydrothermal carbonization of digested sewage sludge

J.D. Marin-Batista, A.F. Mohedano, J.J. Rodríguez, M.A. de la Rubia\*

Chemical Engineering Department, Universidad Autonoma de Madrid, Campus de Cantoblanco, 28049, Madrid, Spain.

\*angeles.delarubia@uam.es

## Abstract

This work evaluates the potential of hydrothermal carbonization (HTC) to valorise the digestate derived from sewage sludge into useful materials for P and energy recovery. The hydrothermal treatment of digestate at 180 – 240 °C did not lead to high-rank hydrochars. On the other hand, inorganic P concentration did not change with the temperature, while as the carbonization temperature increased, the organic P retention yield in hydrochar became lower, increasing the total P in the process water obtained at the highest temperature, up to 25.3%. P recovery from acid leaching of the hydrochar obtained at 180 °C, via precipitation with CaO at pH up to 9, led to a brown solid precipitate with total P content close to 42 mg g<sup>-1</sup>, in the range of low grade phosphorus ores. Moreover, acid leaching reduced by 50% the ash content, yielding lignite-like upgraded hydrochars with higher heating values in the range of 20.5 – 23.1 MJ kg<sup>-1</sup>, fairly interesting as solid fuels. Anaerobic digestion of the process water enabled additional energy recovery in form of biogas (325 and 279 mL CH<sub>4</sub> g<sup>-1</sup> VS -at standard temperature and pressure; STP- from the process water resulting at 180 and 210 °C, respectively).

**Keywords:** anaerobic digestion; digestate; hydrothermal carbonization; phosphorus recovery

## 1. INTRODUCTION

Anaerobic digestion (AD) is often implemented in wastewater treatment plants (WWTP) for sewage sludge stabilization due to the added-value of energy recovery in the form of biogas (Kacprzak et al., 2017). Depending on the size and configuration of the WWTP, the recovered energy can offset 40 – 75% of the total power consumed on-site (Silvestre et al., 2015). Thus, in 2016 more than 2,800 WWTPs contributed with almost 1.4 Mtoe ( $\approx 16.3 \cdot 10^6$  MWh) to the European Union (EU) electricity production, about 400 ktoe ( $\approx 4.6 \cdot 10^6$  MWh) higher than the 2009 figure (EBA, 2017; EurObserv'ER, 2017). However, the suitability of AD relies on the ability of the WWTPs operators to manage the digested sewage sludge (digestate) (Aragón-Briceño et al., 2017).

Digestate landfilling is being less and less used owing to more stringent EU environmental regulation (Kacprzak et al., 2017). From the circular economy perspective (European Commission, 2018), digestate is managed via two major routes: nutrient reclamation by composting and energy recovery by incineration (Kleemann et al., 2017; Vardanyan et al., 2018). However, the high content of heavy metals (e.g., Al, Cr, As, Ni, and Hg) would make both practices no longer suitable (Wang et al., 2019). Heavy metals, along with other undesirable substances (e.g., inorganic nitrogen, toxic organic compounds or endocrine disruptors) limit the use of digestate for land-application to rates below  $6 \text{ ton ha}^{-1} \text{ year}^{-1}$  (Dragicevic et al., 2018). Even, some European countries (e.g. Netherlands, Romania, and Slovakia) have banished this practice since the long-term impact of heavy metals on plant yields and soil biological activity is still unknown

(Kacprzak et al., 2017). On the other hand, incineration turns digestate nutrients and heavy metals into ashes that agglomerate in combustion chambers to an extent of depleting thermal efficiency (Kratzeisen et al., 2010). Moreover, ashes from incineration are disposed in landfills, ignoring their significant potential to be used as a secondary source of P (8.9–35.9% of  $P_2O_5$ , within the range of phosphate ores) for the manufacture of fertilizers and phosphoric acid (Mar and Okazaki, 2018; Wang et al., 2018).

Separation of desirable from undesirable substances in digestate is therefore of high interest and technologies are developing fast, especially for P recovery (Becker et al., 2019). In this context, hydrothermal carbonization (HTC) is a thermochemical process able to treat wet biomass within the temperature range of 180 – 250 °C and the corresponding equilibrium pressure (2 – 10 MPa) (Zhao et al., 2018), yielding a solid so-called hydrochar and a process water (PW) of high organic load. HTC has evolved as an environmentally friendly and energy-efficient sustainable technology (Zhao et al., 2014). In general, hydrochars derived from digestate show fairly interesting higher heating values (HHVs) in the range of 14 – 16 MJ kg<sup>-1</sup>, which make them attractive for coal co-firing (Aragón-Briceño et al., 2017). Moreover, HTC improves significantly the dewaterability of the resulting solid (Kim et al., 2014), remove harmful substances (endocrine disruptors, pathogens and other microorganism) (Wang et al., 2019) and convert organic pollutants through typical carbonization reactions (hydrolysis, decarboxylation, dehydration, polymerization, and condensation) (Rodriguez Correa et al., 2017). Process conditions (temperature, retention time and pH) can be conveniently managed to optimise the hydrochar solid-fuel properties and nutrients retention (P- $PO_4^{3-}$  and N- $NH_4^+$ ), being the optimal conditions for carbonization and nutrient recovery divergent in terms of temperature and pH (Stutzenstein et al., 2018).

76

77 Hydrochar can generally retain over 60% of C, 80% of P, and 40% of N present in the  
78 feedstock (Wang et al., 2017). P is usually in inorganic form (apatite and non-apatite  
79 orthophosphate) and its speciation is strongly related with the presence of Ca, Fe and Al  
80 in the feedstock (Xu et al., 2018). Digestate usually contains high concentrations of Al  
81 and Fe due to the use of iron or aluminium sulphate across WWTP to precipitate  
82 phosphate in the water line and sludge thickening/dewatering systems (Dragicevic et al.,  
83 2018; Silvestre et al., 2015). Therefore, inorganic P tends to stay, even under acidic  
84 hydrothermal conditions, in these very stable metal associations and is fixed in the  
85 hydrochar along with a large amount of other heavy metals (Becker et al., 2019). Finally,  
86 both P and heavy metals can be removed from hydrochars by acid leaching, being P  
87 further reclaimed from leachate by precipitation (Becker et al., 2019; Zhao et al., 2018).

88

89 On the other hand, the PW obtained by HTC of sewage sludge has shown high values of  
90 chemical oxygen demand (COD; 90-110 g L<sup>-1</sup>), including volatile fatty acids (VFAs),  
91 furan compounds, phenols, N-containing species (e.g., ammonia, pyrazines, amines, and  
92 pyrroles), among other components (Villamil et al., 2019, 2018). Taking into account the  
93 biodegradability of many of the components of this fraction, it can be valorised by AD to  
94 obtain additional energy in form of biogas (De la Rubia et al., 2018a). AD allows around  
95 44 – 61% removal of the initial COD in PW, and almost complete removal of furans and  
96 phenols (De la Rubia et al., 2018b). Meanwhile, N-containing species can influence the  
97 anaerobic biodegradability of PW (Chen et al., 2019).

98

99 Despite the apparent advantages of HTC as a post-treatment for digestate, so far many  
100 research works have focused on the hydrochar and PW characteristics regarding potential

use as energy and nutrients source, while only few studies have tried to define valorisation routes addressed to the integral exploitation of HTC within the EU circular economy. Aragón-Briceño et al. (2017) suggested a cascade process for the valorisation of sewage sludge comprising AD followed by HTC as a post-treatment to recover energy from digestate. The energy associated to the hydrochar plus the biogas produced from PW (10.8 – 12.7 MJ kg<sup>-1</sup> feedstock) was significantly higher than the overall energy recovered from the conventional AD of the sewage sludge pre-treated by thermal hydrolysis (7.1 MJ kg<sup>-1</sup> feedstock). Regarding to nutrients recovery, phosphorus can be extracted from the ashes after hydrochar combustion and recycled for its added-value, since the sole use of hydrochar as energy source implies wasting nutrients. Becker et al. (2019) suggested a nutrient recovery approach from digestate HTC implying acid leaching of hydrochars for P recovery (up to 82.5 wt.%) after struvite precipitation and further use of PW as ammonia source (107 – 291 mmol L<sup>-1</sup> NH<sub>4</sub><sup>+</sup>).

The aim of this study is evaluating the potential of hydrothermal carbonization to convert digestate derived from sewage sludge into valuable materials for phosphorus and energy recovery. The suggested valorisation route implied two stages (i) phosphorus reclamation by acid leaching of hydrochar and (ii) energy recovery by coupling combustion of leached hydrochars and anaerobic digestion of PW.

## **2. MATERIAL AND METHODS**

### **2.1 Hydrothermal carbonization of digestate**

Dewatered digestate (83.5 ± 5% moisture content), containing 165 ± 1.2 g kg<sup>-1</sup> of total solids (TS), 103 ± 3 g kg<sup>-1</sup> of volatile solids (VS), and 852 ± 8 g O<sub>2</sub> kg<sup>-1</sup> of total COD

(TCOD), was collected from a WWTP, located in central Spain, processing sewage sludge in a mesophilic anaerobic reactor.

HTC tests were performed at 180, 210 and 240 °C in an electrically heated 4 L ZipperClave® pressure vessel. The vessel was loaded with 2 kg of digestate on wet basis. The operating temperature for the HTC runs was reached at a heating rate of 3 °C min<sup>-1</sup> and then held for 1 h. The reaction was quenched by cooling with an internal heat exchanger using tap water. The slurry (hydrochar and PW) was separated by vacuum filtration (0.90 µm), then the supernatant was filtered (0.45 µm) and the PW obtained was stored (4 °C) for using as substrate in the AD tests.

The hydrochar (HC) was oven-dried overnight at 105 °C, and then ground and sieved. A Filtra No. 38373 sieve was used to separate the hydrochar into three fractions, namely:  $\emptyset > 0.5$  mm;  $0.25 < \emptyset < 0.5$  mm and  $\emptyset < 0.25$  mm, being the smallest one used for characterization. The hydrochars obtained were labelled as HC180, HC210, and HC240, related to the HTC temperature used. Thereafter, acid leaching of hydrochars (particle size,  $\emptyset < 0.25$  mm) was carried out in order to remove inorganic components. The acid leaching was performed with 1 N HCl (50 mL g<sup>-1</sup> hydrochar) in a Soxhlet extractor for 2 h and repeated two more times (total extraction time, 6 h) (Marin-Batista et al., 2019). The leached hydrochars, from now onwards called upgraded hydrochars (UHC), were washed with deionized water until neutral pH and then oven-dried overnight at 105 °C. The resulting upgraded hydrochars were labelled as UHC180, UHC210, and UHC240.

## **2.2 Phosphorus speciation and reclamation**

The P species in solid phase, digestate and hydrochars, were analysed according to the Standards in Measurements and Testing (SMT) extraction protocol (Zhao et al., 2018).

The extraction protocol enabled to identify:

(a) Inorganic P (IP), extracted by mixing 0.2 g solid sample with 20 mL of 1 N HCl under continuous stirring for 16 h at 25 °C.

(b) Organic P (OP), obtained by calcination of the residual solid after IP extraction at 450 °C for 3 h, and then treating ashes with 20 mL of 1 N HCl under continuous stirring for 16 h at 25 °C.

(c) Non-apatite IP (NAIP), the P associated with Al, Fe, Mg, and Mn oxides and hydroxides, extracted by mixing 0.2 g solid sample with 20 mL of 1 N NaOH under continuous stirring for 16 h at 25 °C. Thereafter, 10 mL of extract was mixed with 4 mL of 3.5 N HCl for 16 h at 25 °C without stirring.

(d) Apatite P (AP), the P species associated with Ca. Extracted by mixing 0.2 g solid sample with 20 mL of 1 N NaOH under continuous stirring for 16 h at 25 °C. Thereafter, the solid residue was treated with 20 mL of 1 N HCl under continuous stirring for 16 h at 25 °C.

Therefore, total P was calculated as follows:

$$Total\ P\ (TP) = IP + OP, \text{ where } IP = NAIP + AP.$$

Phosphate was determined from the supernatant solutions following spectrophotometric method based on the formation of vanadium-molybdenum phosphate (APHA, 2005). The concentrations of phosphate species were expressed in terms of phosphorus retention yield (g PO<sub>4</sub><sup>3-</sup> per 100 g TP feedstock) given by Eq. (1):

$$Phosphorus\ retention\ yield = Y_{HC,UHC,PW} \cdot \left( \frac{P_y}{TP_{feedstock}} \right) \cdot 100 \quad (1)$$



Where,  $P_y$  represents each species of the four P fractions (IP, OP, AP and NAIP) measured for each HC.  $TP_{feedstock}$  corresponds to the TP concentration in digestate.  $Y_{HC,UH,PW}$  corresponds to HTC-product mass yields calculated according to Eq. (2). The mass yields of hydrochar ( $Y_{HC}$ ) and upgraded hydrochar ( $Y_{UHC}$ ) were defined as the respective weight ratio of recovered hydrochar ( $W_{HC}$ ) and upgraded hydrochar ( $W_{UHC}$ ) to digestate ( $W_D$ ) fed into the HTC reactor, on a TS basis. Similarly, process water mass yield ( $Y_{PW}$ ) is the weight ratio between of recovered PW ( $W_{PW}$ ) to digestate ( $W_D$ ) fed, also on a TS basis.

$$Y_{HC,UHC,PW}(\%) = \left( \frac{W_{HC,UHC,PW}}{W_D} \right) \cdot 100 \quad (2)$$

After acid leaching of HC180, HC210, and HC240, the resulting leachates were used for P recovery via precipitation with CaO. The procedure involves addition of 0.5 M CaO to 25 mL of acid leachate (previously filtered through a 0.22  $\mu\text{m}$  membrane) in 250 mL Erlenmeyer flasks, until reaching a pH of 5, 7, and 9. The mixtures were stirred at 80 rpm in a thermostatic shaker at room temperature. Addition of CaO to the acid leachate caused precipitation of a brown solid. The corresponding solids were separated by filtration through a 0.22  $\mu\text{m}$  membrane, washed with deionized water and characterized by inductively coupled plasma atomic emission spectroscopy (ICP-MS).

### 2.3 Anaerobic digestion experiments

Anaerobic digestion runs of PW and digestate were carried out batchwise in 120 mL glass serum vials. The initial inoculum concentration was set at 15 g VS  $\text{L}^{-1}$  and the inoculum-to-substrate ratio (ISR) at 2:1 on a VS basis. The inoculum used was a granular anaerobic sludge from an industrial digester processing brewery wastewater under mesophilic

conditions (35 °C), and was selected based on the results obtained comparing different inocula in the anaerobic digestion of PW from HTC process (de la Rubia et al., 2018b). The inoculum showed the following characteristics: pH  $7.2 \pm 0.2$ ;  $80.7 \pm 2.1$  g TS L<sup>-1</sup>;  $70.9 \pm 1.5$  g VS L<sup>-1</sup> and  $70.7 \pm 1.7$  g O<sub>2</sub> L<sup>-1</sup> of TCOD. A basal medium containing macro- and micronutrients prepared and dosed as described elsewhere (Villamil et al., 2018) was added, after which the reaction volume was made up to 60 mL with deionized water. The vials were sealed with rubber stoppers and metallic crimps and then the unfilled space of the vial (60 mL) was purged with N<sub>2</sub> for 3 min to ensure anaerobic conditions. Finally, the vials were held in a thermostatic shaking water bath at 80 rpm equivalent stirring and mesophilic temperature ( $35 \pm 1$  °C).

The time course of AD was followed by using ten vials for each of the PW samples obtained at the three HTC temperatures tested (PW180, PW210, PW240) and for the digestate. Seven of them were sacrificed: two during the first three days and then every week. The remaining three vials were used for tracking the methane production. Triplicate blank samples with no substrate were run to determine the background methane from the inoculum. The methane released was measured by volume displacement (the carbon dioxide was removed previously by flushing the gas through a 2 N NaOH solution) and expressed at standard temperature and pressure (STP; 273.14 K, 1 bar) conditions. Methane production was monitored daily and calculated by subtracting the amount of methane produced by the blank controls from the methane production of each fed reactor. In addition, triplicate control experiments with starch (Panreac) as only substrate were also conducted to verify the inoculum activity.

## 2.4 Quantification of the net energy production

The values of specific methane yield (SMY) obtained in the anaerobic tests were converted into HHV by Eq. (3):

$$HHV_{PW}(MJ\ kg^{-1}) = 39.8 \cdot SMY \cdot \left(\frac{VS}{TS}\right) \quad (3)$$

Where, *SMY* refers to the specific methane yield. The *VS to TS ratio* corresponds to the substrate added into the anaerobic reactor, and 39.8 is the higher heating value of pure methane in MJ Nm<sup>-3</sup>.

The total energy associated to HTC products was calculated by equation (4):

$$Energy\ produced\ (MJ\ kg_{feedstock}^{-1}) = HHV_{HC,UHC} \cdot Y_{HC,UHC} + HHV_{PW} \cdot Y_{PW} \quad (4)$$

Where, *HHV<sub>HC,UHC</sub>* corresponds to the HHV (MJ kg<sup>-1</sup>) of hydrochars and upgraded hydrochars, respectively.

## 2.5 Analytical methods

The dried solid samples (digestate, hydrochars, and upgraded hydrochars) were analysed by elemental composition determined with a CHNS analyser (LECO CHNS-932, Model 601-800-500), using the manufacturer's standard procedures. Proximate analysis (ash, fixed carbon (FC) and volatile matter (VM)) was done by thermogravimetric analysis (TGA) according to ASTM D7582 (ASTM, 2015). The HHV of solid samples were determined by using an IKA C2000 bomb calorimeter according to technical specification

EN 15400 (EN 15400:2011, 2011). Major elements in ashes were analysed by ICP-MS with an Elan 6000 Sciex instrument (Perkin Elmer).

The raw digestate, PWs and the inoculum were characterized by measuring pH with a Crison 20 Basic pH-meter; TS and VS according to standard methods 2540B and 2540E, respectively (APHA, 2005) and total organic carbon (TOC) in a Shimadzu TOC-VCPN auto analyser. Total Kjeldahl nitrogen (TKN) was determined as described elsewhere (Villamil et al., 2018) and the TCOD according to Raposo et al. (2008). PWs and sacrificed samples from the AD tests (centrifuged and filtered through a filter of 0.45 µm pore size) were analysed as follows: Soluble COD (SCOD) according to standard method 5220D (APHA, 2005); carbohydrates by colorimetric method (Dubois et al., 1956); proteins by the Lowry method (Lowry et al, 1951); total alkalinity (TA) by titration to pH 4.3 with 0.02 N H<sub>2</sub>SO<sub>4</sub> and total ammonia nitrogen (TAN) by distillation and titration according to standard methods 2320B and 4500-NH<sub>3</sub>, respectively (APHA, 2005). The concentrations of individual volatile fatty acids (VFAs) from acetic to heptanoic, iso-forms included, were determined by gas chromatography (GC) in a Varian 430-GC instrument equipped with a flame ionization detector (FID) and a capillary column filled with Nukol (nitroterephthalic acid-modified polyethylene glycol) (De la Rubia et al., 2018b). Chemical species were identified in a GC-MS CP-3800/Saturn 2200 instrument equipped with a Varian CP-8200 autosampler injector (De la Rubia et al., 2018a).

### **3. RESULTS AND DISCUSSION**

#### **3.1 Characteristics of digestate and hydrochars**

273 Representative analyses of digestate, HCs, and UHCs are shown in Table 1. As can be  
274 seen from the elemental composition of the virgin hydrochars (HC samples), the  
275 hydrothermal treatment did not lead to significant carbonization. The higher relative C  
276 content of the UHC results from partial removal of the inorganic fraction (ash) by acid  
277 leaching. Only at the highest HTC temperature some moderate carbonization took place,  
278 as can be concluded from the comparison of the C content of the starting digestate and  
279 the HC240 hydrochar on ash-free basis (55.3 and 62.8%, respectively).

Table 1. Characteristics of digestate, hydrochars, and upgraded hydrochars (dry basis).

	Digestate	HC180	HC210	HC240	UHC180	UHC210	UHC240
C (%)	32.7	30.8	31.8	32.6	50.1	52.5	55.8
H (%)	4.9	4.3	4.3	4.1	5.9	5.9	6.0
N (%)	5.1	4.2	4.1	4.1	5.2	5.0	4.7
S (%)	1.0	1.0	1.0	1.1	1.4	1.5	1.5
O (%)*	15.4	16.8	14.9	10.0	14.7	15.3	5.2
VM (%)	54.7	50.9	48.3	44.0	60.9	59.4	55.3
FC (%)	4.4	6.2	7.8	7.9	16.4	20.8	17.9
Ash (%)	40.9	42.9	43.9	48.1	22.7	19.8	26.8
HHV (MJ kg <sup>-1</sup> )	14.9	14.7	14.9	15.1	20.5	21.6	23.1
Yield (%)	-	74.2	67.8	51.8	64.4	57.3	44.3

Note: Each data showed a standard deviation  $\leq 0.2$

\*By difference

1 The main issues with ash are potential risks for slagging and fouling in the furnace upon  
2 combustion, which is related to ash composition rather than its amount (Kratzeisen et al.,  
3 2010). Most furnaces are designed to remove ash as a powdery residue and then, having  
4 ash with high melting-temperature is desirable. Alkaline metals, potassium and sodium,  
5 reduce the ash melting temperature, while magnesium and calcium have the opposite  
6 effect (Smith et al., 2018). During the HTC process, alkaline metals responsible for  
7 fouling are generally dissolved into the PW (Yang et al., 2019). These elements seem to  
8 have high affinity with the PW (Wang et al., 2019), but this is not the case for the digestate  
9 herein studied because the content of alkaline metals and even magnesium in HCs scantily  
10 varied respect to digestate, as can be seen in Table 2, which discloses the major elements  
11 in the ash fraction. The most abundant elements in the digestate ash correspond to P, Al,  
12 Ca, Si, and Fe, which accumulate in the HCs in higher extent at increasing HTC  
13 temperature (Table 2). This can be associated with the interaction of  $P-PO_4^{3-}$  with  
14 dissolved metallic cations and ammonia in PW to form precipitated phosphate salts onto  
15 the hydrochar surface (Becker et al., 2019). The higher amount of carboxylic groups on  
16 the hydrochar surface at increasing HTC temperature can theoretically enhance the cation  
17 exchange capacity (Kim et al., 2014). However, the diversity of metal species in the HCs  
18 can provoke some problems. During combustion of the HCs herein obtained, alkaline  
19 metals might actively interact with Al, Si, and Fe giving rise to eutectic mixtures lowering  
20 the ash melting temperature (Yang et al., 2019). Thus, ash removal would not only  
21 increase the heating value of the hydrochars but also reduce the problems derived from  
22 slagging in the combustor.

23  
24 After acid washing, all HCs showed a mass loss of around 15%, due to ash leaching. This  
25 led to recovery yields of 64.4, 57.3, and 44.3% for UHC180, UHC210, and UHC240,

respectively (Table 1). The reduction of ash content was about 50% for all the HCs, consequently leading to higher values of fuel ratio (FC/VM) in the UHCs, which were around double than those of the corresponding virgin HCs. This increase of the fuel ratio represents an improvement of fuel quality since higher FC values help to control the heat loss caused by an unstable flame, typically exhibited by solid fuels with high VM content (Marin-Batista et al., 2019). FC increased along with carbon content by a factor of approximately 2.5, which augmented around 1.5 fold the HHVs initially obtained from hydrochars untreated with HCl. In addition, oxygen content decreased due to dissolution of certain O-containing species into the acid washing solution, like hydroxides, organic acids or phenols from the hydrochar (Zhao et al., 2018). Consequently, H/C and O/C molar ratios comparable to those of lignite were achieved.

Table 2. Major elements in the ash fraction of digestate, hydrochars, and upgraded hydrochars (dry wt. %).

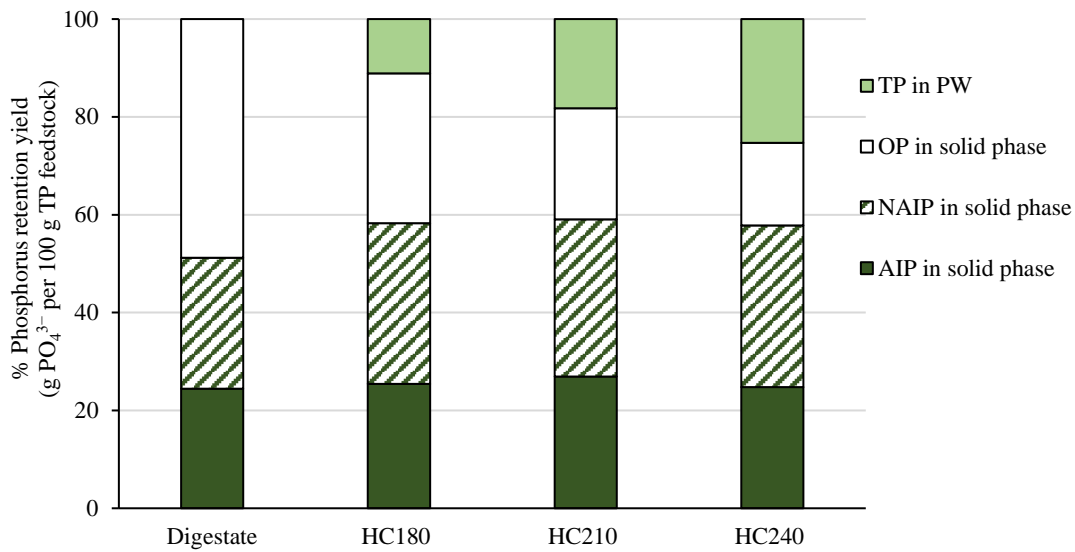
Element	Digestate	HC180	HC210	HC240	UHC180	UHC210	UHC240
K	0.28	0.27	0.26	0.35	0.16	0.14	0.13
Na	0.16	0.14	0.14	0.18	0.01	0.01	0.01
Mg	0.32	0.33	0.34	0.45	0.09	0.04	0.01
Ca	3.02	3.28	3.23	3.98	0.02	0.01	0.01
Si	1.94	1.85	2.24	2.68	0.03	0.02	0.01
Fe	1.58	1.74	1.78	2.21	0.38	0.33	0.30
Al	4.19	3.84	4.14	5.57	0.97	0.89	0.91
P	4.58	5.28	5.32	6.30	0.06	0.03	0.02

Note: Each data showed a standard deviation below  $\pm 0.01$

### 3.2 Phosphorus reclamation

During the hydrothermal treatment, the TP of digestate (45.8 mg g<sup>-1</sup>, Table 2) was split into the HTC fractions (HC and PW). Fig. 1 shows the changes in P species (NAIP, AIP, and OP) upon the hydrothermal treatment.





46

47 Figure 1. Distribution of the initial P of digestate into the hydrochars and process water  
48 from HTC.

49

50 As the HTC temperature increased, the TP retention yield in PW became higher, reaching  
51 percent values of 11.1 (PW180), 18.2 (PW210), and 25.3 (PW240). This is due to higher  
52 dissolution of organic matter to the PW. Oppositely, OP retention yields in digestate  
53 (48.8%) declined until 30.6 (HC180), 22.7 (HC210), and 17.9% (HC240). This finding  
54 draw the conclusion that under HTC conditions the OP of digestate was released into the  
55 PW as ortho-phosphate, wherein most likely reacted with  $Mg^{2+}$ ,  $Al^{3+}$ , and  $Fe^{3+/2+}$  to  
56 increase NAIP retention yield in the solid from 26.8% (digestate) to around 33% for the  
57 hydrochars obtained at different temperatures. Meanwhile, digestate AIP retention yield  
58 of 24.5% scarcely varied during the hydrothermal treatment (Fig. 1), because a Ca/P  
59 molar ratio of 0.5 kept constant regardless the HTC temperature (Table 2). Interestingly,  
60 very diverse findings have been reported in literature. For instance, Zhao et al. (2019)  
61 concluded that HTC partially turns OP and NAIP from lignocellulosic digestate into AIP  
62 in the PW, likely through a sequential reaction including the hydrolysis of OP, the

dissolution of NAIP and the precipitation of phosphate with  $\text{Ca}^{2+}$  and/or hydroxyl groups. However, Wang et al. (2017) stated that an acidic reaction environment promotes the transformation of AIP to NAIP, while an alkaline environment provokes the opposite. Certainly, HTC promoted the transformation of digestate OP into IP, and IP speciation during HTC may be linked to the amount and composition of inorganic elements in the feedstock.

Nonetheless, the vast majority of TP content of HC was released by acid leaching along with a large fraction of multivalent and monovalent metals, as can be concluded from Table 2. Despite P and metals content varied among acid leachates (data not shown), close to 100% of dissolved TP was precipitated in form of brown solids by addition of CaO. Fig. 2 shows the content of major elements in brown solids precipitated from HC180 acid leachate. As pH increases upon CaO addition, P content in the brown solids increased from  $\approx 10.5 \text{ mg g}^{-1}$  at pH 5 to  $\approx 42 \text{ mg g}^{-1}$  at pH 9, which is comparable to the P content of low grade phosphate ores ( $26.5 - 163.5 \text{ mg g}^{-1}$ ) (Mar and Okazaki, 2018). Considering that different phosphorus chemical species (e.g.,  $\text{H}_2\text{PO}_4^-$ ,  $\text{HPO}_4^{2-}$ , and  $\text{PO}_4^{3-}$ ) occur within a pH range of 5 to 9 (Vardanyan et al., 2018) and due to the abundance of Ca in brown solids (Fig. 2), different apatite species could precipitate due to calcium base neutralisation. From a thermodynamic point of view, hydroxyapatite ( $\text{Ca}_{10}(\text{PO}_4)_6(\text{OH})_2$ , Ca/P of 1.67) precipitation should dominate since it is the most stable bonding form of calcium and orthophosphate ions (Cichy et al., 2019). However, a Ca/P molar ratio of 0.60 was barely achieved in the pH range of 7 to 9. Possible phosphate precipitates are heptacalcium phosphate ( $\text{Ca}_7(\text{P}_5\text{O}_{16})_2$ ; Ca/P of 0.70), tetracalcium dihydrogen phosphate ( $\text{Ca}_4\text{H}_2\text{P}_6\text{O}_2$ ; Ca/P of 0.67), monocalcium phosphate monohydrate ( $\text{Ca}(\text{H}_2\text{PO}_4)_2 \cdot \text{H}_2\text{O}$ ; Ca/P of 0.50), and calcium metaphosphate ( $\text{Ca}(\text{PO}_3)_2$ ; Ca/P of 0.50). The leaching

conditions (i.e., pH, mixing time) and stoichiometric relation between P and metal ions ( $\text{Al}^{3+}$ ,  $\text{Fe}^{2+/3+}$ ,  $\text{Mg}^{2+}$ ,  $\text{K}^+$ , and  $\text{Na}^+$ ) in leachates, may lead to precipitation of different phosphate salts that somewhat interfere with the formation of apatite species. Despite the conditions for hydroxyapatite precipitation were not optimal, the side reactions of phosphate with the metal ions in the leachate implied lower needs of calcium to achieve complete recovery of P from the acid leachates. The phosphate species in brown solids have a very low solubility which impedes direct use as fertilizer, but that solid product can be used for phosphoric acid production.

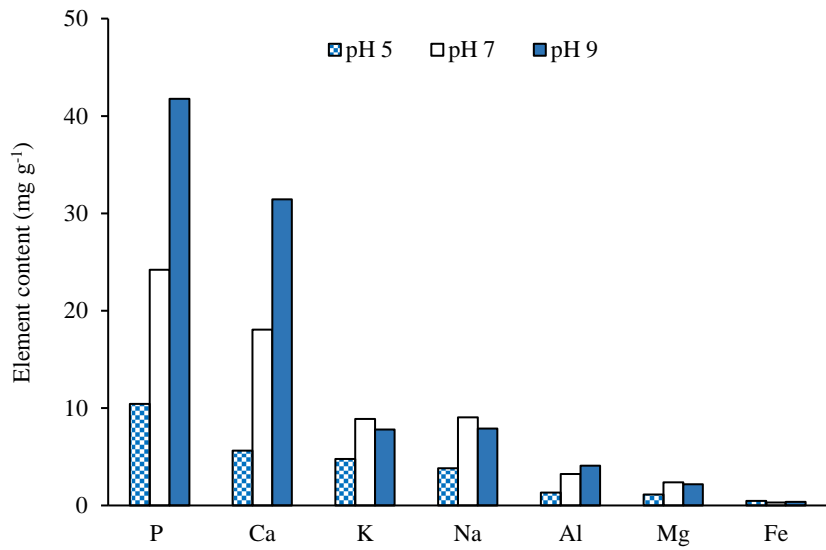


Figure 2. Content of major elements in the brown solid precipitated from HC180 acid leachate.

### 3.3 Characteristics of the process water

The characteristics of the PWs obtained by digestate HTC are collected in Table 3. Increasing the HTC temperature leads to higher dissolution of total and volatile solids from the starting digestate. This fact could be perceived as a subsequent increase of SCOD in the PW. However, the SCOD showed a downward trend from 61.5 to 53.9 g L<sup>-1</sup> after increasing the HTC temperature from 210 to 240 °C. This reduction in SCOD can be

related to the significant decomposition of proteins and carbohydrates at higher HTC temperature. It has been reported that dehydration is the major reaction during HTC of sewage sludge, while deamination and hydrolysis occur significantly at higher HTC temperature or longer residence time. Particularly, proteins are hydrolysed to peptides and amino acids, which in turn are oxidatively degraded to fatty acids and ammonia, leading to increased alkalinity (Chen et al., 2019). Significantly high content of proteins were found in PW180, but decreased as the HTC temperature increased. The same trend was observed for total VFA (TVFA). Thus, ammonia, TA, and pH of PW increased with HTC temperature.

Table 3. Analysis of the process water from HTC of digestate at different temperature.

	PW180	PW210	PW240
Total solids (g L <sup>-1</sup> )	52.2 (0.2)	46.3 (0.9)	30.1 (0.5)
Total volatile solids (g L <sup>-1</sup> )	50.3 (0.1)	44.6 (0.1)	28.9 (0.1)
Soluble chemical oxygen demand (g L <sup>-1</sup> )	56.2 (0.8)	61.5 (0.3)	53.9 (0.2)
pH	7.4 (0.1)	7.9 (0.2)	8.9 (0.1)
Total alkalinity (g CaCO <sub>3</sub> L <sup>-1</sup> )	1.1 (0.1)	2.6 (0.1)	3.2 (0.1)
Total organic carbon (g L <sup>-1</sup> )	28.8 (0.2)	28.3 (0.1)	25.9 (0.1)
Total Kjeldahl nitrogen (g L <sup>-1</sup> )	8.1 (0.2)	9.0 (0.1)	9.7 (0.2)
Total carbohydrates (g L <sup>-1</sup> )	7.6 (0.1)	2.8 (0.1)	0.6 (0.1)
Total proteins (g L <sup>-1</sup> )	11.7 (0.2)	11.0 (0.1)	9.8 (0.4)
Total ammonia nitrogen (g L <sup>-1</sup> )	4.9 (0.2)	5.2 (0.1)	6.3 (0.2)
Total volatile fatty acids (g L <sup>-1</sup> )	3.5 (0.2)	3.4 (0.3)	2.0 (0.3)

Note: Standard deviation in parentheses

The carbon balance based on elemental analysis (solid phase) and total organic carbon (liquid phase) matched within 80.2 % (240 °C) and 92.8 % (180 °C). Carbon content in the gaseous stream increased with carbonization temperature. This gaseous phase

contains mainly CO<sub>2</sub> (> 90 %) and small amounts of CH<sub>4</sub>, H<sub>2</sub>, and CO (Cha et al., 2016; Baso et al., 2016). In the case of nitrogen content, analyzed by elemental analysis (solid phase) and total Kjeldahl nitrogen (process water), the same trend was observed. Mass nitrogen balance closure was from 99.2 % (180 °C) to 90.8 % (240 °C). Taking into account the nitrite and mainly nitrate formation the nitrogen mass balance matched within 99.5 % at least.

### **3.4 Anaerobic digestion of process water and digestate**

Fig. 3 shows the time course of the methane yield upon AD of the digestate and PWs resulting from digestate HTC. An initial lag-phase of 3 days was observed in all cases, indicative that the inoculum required some time to adapt to the substrate (De la Rubia et al., 2018b). Then, the methane production reached  $325 \pm 11$  STP mL CH<sub>4</sub> g<sup>-1</sup> VS for PW180 and a lower value ( $279 \pm 9$  STP mL CH<sub>4</sub> g<sup>-1</sup> VS) for PW210. These values were significantly higher than the observed for the digestate ( $150 \pm 1$  STP mL CH<sub>4</sub> g<sup>-1</sup> VS). The increase in carbonization temperature showed a negative effect on the anaerobic biodegradability of the resulting PW, which was dramatic for the PW generated at 240 °C where methane production barely took place. The results are useful regarding the possibility to recirculate the HTC process water inside the digester. The ratio between the mass of input entering the digester and the mass of HTC process water should be established in long-term experiments, and the possible remaining process water could be treated with the wastewater entering in the treatment plant.

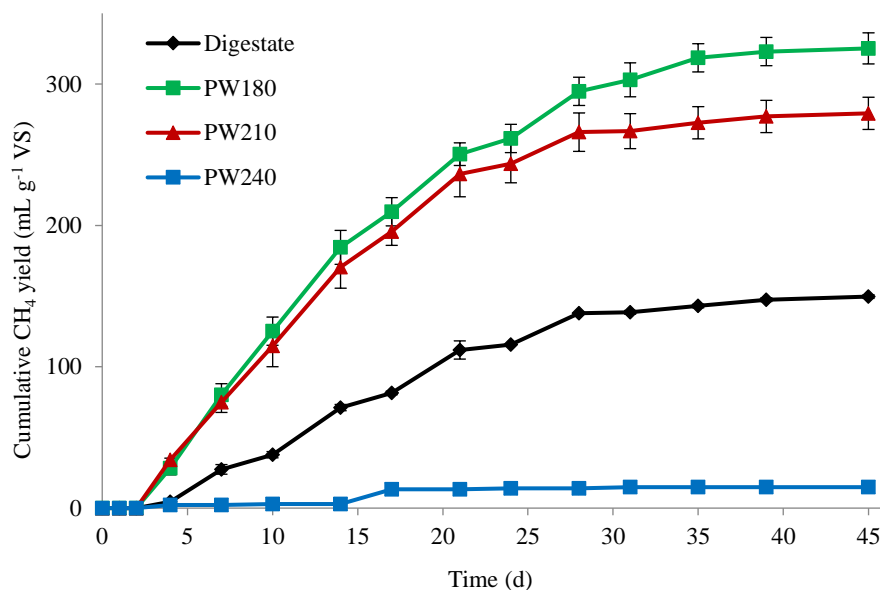


Figure 3. Time course of cumulative methane yield from AD of process waters and digestate.

Methanogenic microorganisms use SCOD in the form of VFA, specifically as acetic acid, for methane production. Therefore, the time course of individual VFA (Fig. 4) can provide useful information on the performance of the acidogenesis and methanogenesis stages of AD. In the early stages acetic acid (C2) was by far the major VFA produced, while longer chain VFAs such as valeric (C5) and iso-valeric (i-C5) were present in low concentrations ( $< 100$  mg acetic acid L<sup>-1</sup>). A similar VFA profile was observed by Chen et al. (2019) in the anaerobic digestion of the PW derived from sewage sludge HTC. VFA are easily-biodegradable compounds and the metabolic pathway of individual VFA was influenced by the HTC temperature (Fig 4). During the AD of PW180 and PW210, the concentration of C3 and i-C5 gradually decreased due to the effective acidogenic – acetogenic stage, wherein VFAs are turned into C2. Remarkably, C4 and i-C4 were rapidly converted into C2 during the first week, confirming that C4 and i-C4 conversion is favoured within the VFA metabolic pathway. At the end of the experiment, the TVFA concentration (expressed as mg acetic acid L<sup>-1</sup>) in the cases of PW180 and PW210 was,

respectively,  $316 \pm 7 \text{ mg L}^{-1}$  (accounting for TVFA reduction of 70%) and  $376 \pm 20 \text{ mg L}^{-1}$  (accounting for TVFA reduction of 60%). This notable reduction of the VFAs concentration demonstrates that the methanogenic stage was not disturbed and the formation of methane from acetate was fairly rapid after the lag period. In contrast, the early inhibition of methanogens during the AD of PW240 led to accumulation of C2 along the digestion time (increasing from the initial concentration of  $612 \text{ mg C2 L}^{-1}$  to  $1266 \text{ mg C2 L}^{-1}$  at the end of the experiment). Herein, C4 and i-C4 were rapidly converted into C2 while methanogens were unable to remove C2 fast enough. This imbalance in acetate production/uptake reaction rates somehow affected to C3 and i-C5 metabolic pathway, leading to accumulation of these species. Thus, TVFA concentration rose up to  $\approx 1900 \text{ mg acetic L}^{-1}$ , comprising mainly 67.1% C2, 12.1% C3, and 17.8% i-C5. Therefore, there should be some inhibiting compounds in the PWs that substantially contributed to inhibition of methanogenesis and low methane yields in the case of PW240.

TVFA evolution (Fig. 4) and significant AD variables such as pH, TA, and TAN allow evaluating the AD process (De la Rubia et al., 2011). For each PW the pH slightly varied (from 8.0 – 8.5 to 7.8 – 7.6) because the alkalinity of the system prevents higher pH drops, associated to VFA accumulations during AD. TA was initially  $\geq 1.5 \text{ mg CaCO}_3 \text{ L}^{-1}$  in all cases but increased up to  $6.0 \text{ g CaCO}_3 \text{ L}^{-1}$  for PW180 and PW210 and  $3.8 \text{ g CaCO}_3 \text{ L}^{-1}$  for PW240, anyway providing enough buffer capacity (Villamil et al., 2020). PW240 showed the lowest final TA values because part of the alkalinity was likely consumed to neutralise VFA accumulation. Besides, the early inhibition in the case of PW240 lowered down the hydrolysis rate of proteins to an extent that TAN was released to a rate unable to counteract TA deficits. The final TAN to TKN concentration ratio is usually used as a valid index for protein hydrolysis in AD (Villamil et al., 2019). The concentration of TAN

increased along AD, suggesting a growing trend for the hydrolysis of TKN in all cases. However, the final values of TAN to TKN ratio of 1.08 (PW180), 0.92 (PW210), and 0.74 (PW240) indicate that the hydrolytic stage was shorter in the AD of PWs obtained at higher HTC temperatures. The final TAN ranged  $1.3 - 1.4 \text{ g L}^{-1}$  for PW180 and PW210, much lower than the considered inhibitory value for methanogenic microorganisms ( $1.7 \text{ g TAN L}^{-1}$ ) (Villamil et al., 2019). Meanwhile, the final TAN in the case of PW240 reached  $1.9 \pm 0.1 \text{ g L}^{-1}$ , slightly higher than the aforementioned inhibitory value. Moreover, the removal of SCOD upon anaerobic digestion decreased as the temperature of HTC increased (46.2 and 38.1% for PW180 and PW210, respectively), being this fact much more significant for PW240, consistently with the accumulation of VFA. The remaining SCOD can be assigned to refractory compounds formed during the hydrothermal treatment, as previously found by Villamil et al. (2018) for AD of PW from sewage sludge HTC.



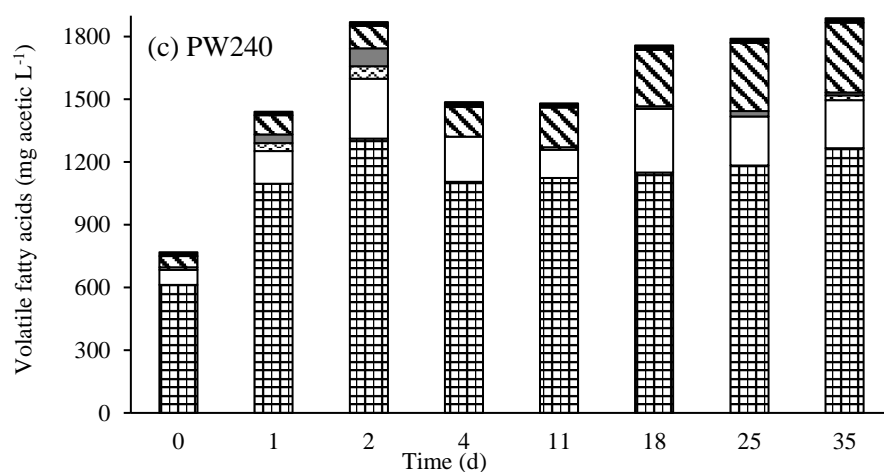
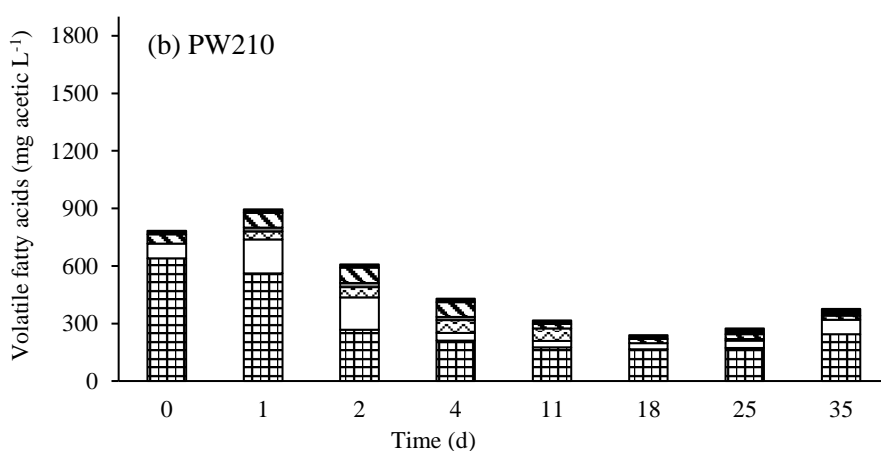
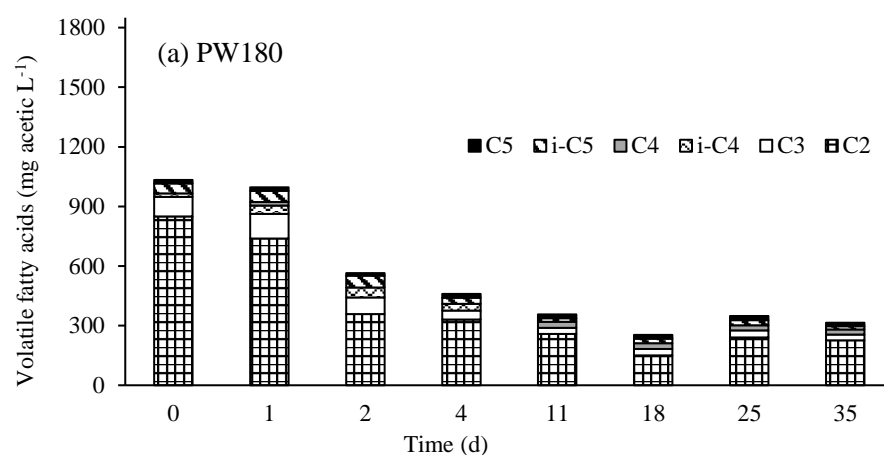


Fig 4. Time course of the relative distribution of individual components of the total volatile fatty acids fraction (expressed as equivalent acetic acid) upon AD of PWs.

### 3.5 Analysis of refractory compounds

Figure A1 (appendix 1) shows the semi-quantitative composition of PW180, PW210 and PW240 before and after AD. The species have been gathered in chemical groups and their concentrations are expressed in terms of % GC peak area. Higher HTC temperature led to a wider diversity of nitrogen-bearing species in the PW. The PW180 showed the presence of ring-type structures with one or two N heteroatoms, such as amines (e.g., trimethylamine, 1-butanamine, 1,2-benzenediamine), pyrimidines (4-methyl-pyrimidine) and pyrazines (2-ethyl-3-methyl-pyrazine, 2,5-dimethyl-pyrazine, 2,3-diethylpyrazine), which are generally formed during the HTC process from hydrolysis of proteins and carbohydrates (De la Rubia et al., 2018a). Increasing HTC temperature provoked the disappearance of some amine species (e.g., trimethylamine and 1-butanamine) from the PW, due to deamination (Chen et al., 2019), and the appearance of new pyrimidine species (e.g. 4,6-dimethyl-pyrimidine at 210 °C and 3-ethyl-4-methyl-pyrimidine at 240 °C), that showed to be refractory to AD. Some anaerobic biodegradable pyrazine species (e.g., 2,5-dimethyl-pyrazine and 2,5-dimethyl-3-propyl-pyrazine) were detected in PW180 and PW240, while some other (e.g., 2-ethyl-3-methyl-pyrazine and 2,3-diethylpyrazine) identified in all the PWs showed to be refractory to AD. Increasing HTC temperature to 240 °C led to the appearance of nitrogen-bearing aromatic species (1H-pyrrole, 3-ethyl-2,4-dimethyl-ortho-phenylenediamine, 4,5-dimethyl-2-ethylpiperidine) that were completely removed upon AD. Other aromatic species were also detected in all PWs (e.g. 1,3-dioxolane, 1,2,4,5-tetramethyl-benzene, 4-formyl-benzoic acid, 2-methyl-6-(2-propenyl)-phenol, dichloromethyl-benzene). This is generally attributed to the Maillard reactions involving carbohydrate and amino acids as well as cyclization reactions involving alcohols, aldehydes, furans, and pyrroles at high HTC temperatures (Chen et al., 2019). Anaerobic digestion allowed partial removal of the aforementioned aromatic species in all PWs as was previously observed by Villamil et al. (2019) in AD

of PW from sewage sludge HTC. However, new recalcitrant aromatic compounds appeared during AD of PW180 (2,4,6-trimethoxyacetophenone), PW210 (2,3,5,6-tetramethyl-phenol) and PW240 (2,4,6-trimethoxyacetophenone, 7-methyl-1H-indole, and 4-methyl-phenol), accounting for nearly 60% of normalized composition of each PW. The presence of 7-methyl-1H-indole clearly indicates the process inhibition occurred for PW240 as a result of poor digestion, taking into account that this compound can be degraded by methanogens and sulphate-reductive microbial populations (Fisher et al., 2017).

### 3.6 Energy recovery

A value of  $14.9 \pm 0.2 \text{ MJ kg}^{-1}$  (see Table 1) was taken as reference HHV, corresponding to the energy potentially obtained from direct combustion of the digestate feedstock. However, this direct use of digestate as fuel is not recommended (Kratzeisen et al., 2010), due to the high amount of energy required to dry the dewatered digestate ( $2.1 \text{ MJ kg}^{-1}$ ). If the digestate ashes ( $40.9 \pm 0.2 \%$ ) were completely removed, the HHV would be significantly improved (up to  $30.2 \text{ MJ kg}^{-1}$ ), which can give an insight of the maximum amount of energy potentially produced upon combustion of the feedstock after in depth upgrading. However, direct extraction of the digestate ashes would be quite inefficient, since most of the inorganic matter is intracellularly stored and/or entrapped within organic matter (Kleemann et al., 2017).

Fig. 5 shows the energy associated to the combustion of HCs and anaerobic digestion of PW, and also the corresponding to UHCs. The removal of ashes by acid leaching of UHCs, as has been already discussed (see Table 2), allowed a potential way for energy densification of these carbonaceous materials. Coupling combustion of HC180 with AD

of PW180 can provide 14.1 MJ kg<sup>-1</sup> dry feedstock, somewhat higher than the derived from combustion of HC210 plus AD of PW210 (13.5 MJ kg<sup>-1</sup> dry feedstock). These values represent an energy recovery of 94.6 and 90.6% of the energy content of the feedstock. On the contrary, the sole combustion of HC240 would yield only 7.8 MJ kg<sup>-1</sup> dry feedstock, representing 52.3% of the net amount of energy potentially provided by direct digestate combustion. In the case PW240 there is no contribution of anaerobic digestion since the methane yield is negligible. Regarding the upgraded HCs, the combustion of UHC180 and UHC210 could provide 13.2 and 12.3 MJ kg<sup>-1</sup> dry feedstock, which implies 88.6 and 82.6% energy recovery, respectively.

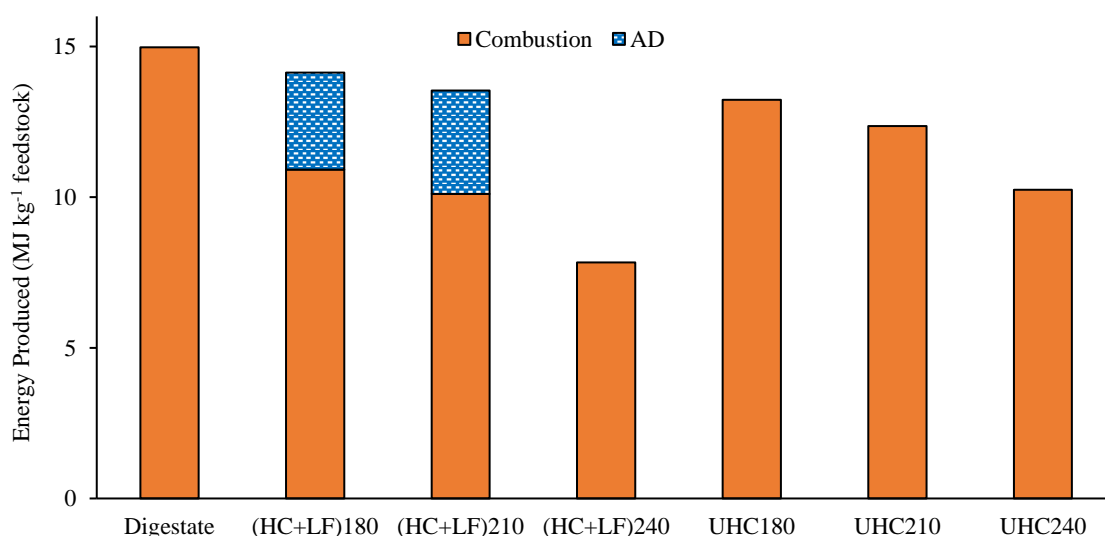


Figure 5. Energy recovery through combustion of hydrochars (HCs and UHC) and anaerobic digestion of PWs.

#### 4. Conclusions

Hydrothermal carbonization provides an interesting way for sewage sludge valorisation into solid fuels, also allowing nutrient recovery. The hydrothermal treatment turns organic P associated to the volatile matter into inorganic P (mainly non-apatite species) from the hydrochars surface. Thus, the vast majority of total P in hydrochars was easily

leached out and can be precipitated in form of brown solids (total P content of 41.8 mg g<sup>-1</sup>, similar to that in a low grade ore) of potential use in the H<sub>3</sub>PO<sub>4</sub> industry.

A mild temperature of 180 to 210 °C is recommended for HTC digestate, in order to obtain hydrochars with attractive HHVs and PWs with relatively low content of refractory compounds to yield additional energy in form of biogas. The energy content of the hydrochars and the methane produced from anaerobic digestion of process water generated at low HTC temperature (180 °C) allows ~95% potential recovery of the energy content in the digestate feedstock. Moreover, this amount of energy in the digestate refers to dry basis and then to be available upon combustion would require the evaporation of high amount of water with the corresponding thermal energy consumption.

## Acknowledgments

Authors greatly appreciate funding from Spain's MINECO (Project CTM2016-76564-R; project RYC-2013-12549) and Madrid Regional Government (Project P2018/EMT-4344). Authors thank to Instituto Colombiano de Crédito Educativo y Estudios Técnicos en el Exterior (Colombia) as part of the grant awarded to José Marin-Batista. The authors thank C.M. Lazaro for her valuable help.

## References

- American Public Health Association, 2005. Standard methods for the examination of water and wastewater, 21<sup>st</sup> ed. Washington, DC, USA. <https://doi.org/30M11/98>
- Aragón-Briceño, C., Ross, A.B., Camargo-Valero, M.A., 2017. Evaluation and comparison of product yields and bio-methane potential in sewage digestate following hydrothermal treatment. Appl. Energy 208, 1357–1369.

<https://doi.org/10.1016/j.apenergy.2017.09.019>

American Society for Testing and Materials, 2015. Standard Test Methods for Proximate Analysis of Coal and Coke by Macro Thermogravimetric Analysis. Method D7582-15. ASTM Int. Pennsylvania.

Basso, D., Patuzzi, F., Castello, D., Baratieri, M., Rada, E.C., Weiss-Hortala, E., Fiori, L., 2016. Agro-industrial waste to solid biofuel through hydrothermal carbonization, Waste Manag. 47, 114–121. <https://doi.org/10.1016/j.wasman.2015.05.013>

Becker, G.C., Wüst, D., Köhler, H., Lautenbach, A., Kruse, A., 2019. Novel approach of phosphate-reclamation as struvite from sewage sludge by utilising hydrothermal carbonization. J. Environ. Manage. 238, 119–125. <https://doi.org/10.1016/j.jenvman.2019.02.121>

Cha, J.S., Park, S.H., Jung, S.-C., Ryu, C., Jeon, J.-K., Shin, M.-C., Park, Y.-K., 2016. Production and utilization of biochar: A review, J. Ind. Eng. Chem. 40, 1–15. <https://doi.org/10.1016/j.jiec.2016.06.002>

Chen, H., Rao, Y., Cao, L., Shi, Y., Hao, S., Luo, G., Zhang, S., 2019. Hydrothermal conversion of sewage sludge: Focusing on the characterization of liquid products and their methane yields. Chem. Eng. J. 357, 367–375. <https://doi.org/10.1016/j.cej.2018.09.180>

Cichy, B., Kuźdzał, E., Krztoń, H., 2019. Phosphorus recovery from acidic wastewater by hydroxyapatite precipitation. J. Environ. Manage. 232, 421–427. <https://doi.org/10.1016/j.jenvman.2018.11.072>

De la Rubia, M.A., Raposo, F., Borja, R., 2011. Influence of particle size and chemical composition on the performance and kinetics of anaerobic digestion process of sunflower oil cake in batch mode. Biochem. Eng. J. 59, 162–167. <https://doi.org/10.1016/j.bej.2011.09.010>

- De la Rubia, M.A., Villamil, J.A., Rodriguez, J.J., Borja, R., Mohedano, A.F., 2018a. Mesophilic anaerobic co-digestion of the organic fraction of municipal solid waste with the liquid fraction from hydrothermal carbonization of sewage sludge. *Waste Manag.* 76, 315–322. <https://doi.org/10.1016/j.wasman.2018.02.046>
- De la Rubia, M.A., Villamil, J.A., Rodriguez, J.J., Mohedano, A.F., 2018b. Effect of inoculum source and initial concentration on the anaerobic digestion of the liquid fraction from hydrothermal carbonisation of sewage sludge. *Renew. Energy* 127, 697–704. <https://doi.org/10.1016/j.renene.2018.05.002>
- Dragicevic, I., Eich-Greatorex, S., Sogn, T.A., Horn, S.J., Krogstad, T., 2018. Use of high metal-containing biogas digestates in cereal production - Mobility of chromium and aluminium. *J. Environ. Manage.* 217, 12–22. <https://doi.org/10.1016/j.jenvman.2018.03.090>
- Dubois, M., Gilles, K.A., Hamilton, J.K., Rebers, P.A., Smith, F., 1956. Colorimetric method for determination of sugars and related substances. *Anal. Chem* 28, 350–356.
- European Banking Authority, 2017. Annual statistical report of the European biogas association. <http://european-biogas.eu>. Last seen on 12/05/2019
- EN 15400:2011, 2011. Solid Recovered Fuels – Determination of Calorific Value. CEN Eur. CS, Brussels.
- EurObserv'ER, 2017. Biogas Barometer. <https://www.eurobserv-er.org/>. Last seen on 14/05/2019
- European Commission, 2018. Directive (EU) 2018/851 of the European parliament and of the council of 30 may 2018 amending directive 2008/98/EC on waste. *Off. J. Eur. union* 109–140.
- Kacprzak, M., Neczaj, E., Fijałkowski, K., Grobelak, A., Grosser, A., Worwag, M., Rorat,

A., Brattebo, H., Almås, Å., Singh, B.R., 2017. Sewage sludge disposal strategies for sustainable development. *Environ. Res.* 156, 39–46.  
<https://doi.org/10.1016/j.envres.2017.03.010>

Kim, D., Lee, K., Park, K.Y., 2014. Hydrothermal carbonization of anaerobically digested sludge for solid fuel production and energy recovery. *Fuel* 130, 120–125.  
<https://doi.org/10.1016/j.fuel.2014.04.030>

Kleemann, R., Chenoweth, J., Clift, R., Morse, S., Pearce, P., 2017. Comparison of phosphorus recovery from incinerated sewage sludge ash (ISSA) and pyrolysed sewage sludge char (PSSC). *Waste Manag.* 60, 201–210.  
<https://doi.org/10.1016/j.wasman.2016.10.055>

Kratzeisen, M., Starcevic, N., Martinov, M., Maurer, C., Müller, J., 2010. Applicability of biogas digestate as solid fuel. *Fuel* 89, 2544–2548.  
<https://doi.org/10.1016/j.fuel.2010.02.008>

Lowry, O.H., Rosebrough, N.J., Farr, Lewis Farr, A., 1951. Protein measurement with the folin phenol reagent. *J. Biol. Chem.* 193, 265–275.  
<http://www.jbc.org/content/193/1/265.citation>

Mar, S.S., Okazaki, M., 2018. Investigation of Cd contents in several phosphate rocks used for the production of fertilizer. *Microchem. J.* 104, 17–21.  
<https://doi.org/10.1016/j.microc.2012.03.020>

Marin-Batista, J., Villamil, J.A., Rodriguez, J.J., Mohedano, A.F., De la Rubia, M.A., 2019. Valorization of microalgal biomass by hydrothermal carbonization and anaerobic digestion. *Bioresour. Technol.* 274, 395–402.  
<https://doi.org/10.1016/j.biortech.2018.11.103>

Raposo, F., De la Rubia, M.A., Borja, R., Alaiz, M., 2008. Assessment of a modified and optimised method for determining chemical oxygen demand of solid substrates and



solutions with high suspended solid content. *Talanta* 76, 448–453.  
<https://doi.org/10.1016/j.talanta.2008.03.030>

Rodriguez Correa, C., Bernardo, M., Ribeiro, R.P.P.L., Esteves, I.A.A.C., Kruse, A.,  
2017. Evaluation of hydrothermal carbonization as a preliminary step for the  
production of functional materials from biogas digestate. *J. Anal. Appl. Pyrolysis*  
124, 461–474. <https://doi.org/10.1016/j.jaap.2017.02.014>

Silvestre, G., Fernández, B., Bonmatí, A., 2015. Significance of anaerobic digestion as a  
source of clean energy in wastewater treatment plants. *Energy Convers. Manag.* 101,  
255–262. <https://doi.org/10.1016/j.enconman.2015.05.033>

Smith, A.M., Whittaker, C., Shield, I., Ross, A.B., 2018. The potential for production of  
high quality bio-coal from early harvested *Miscanthus* by hydrothermal  
carbonisation. *Fuel* 220, 546–557. <https://doi.org/10.1016/j.fuel.2018.01.143>

Stutzenstein, P., Bacher, M., Rosenau, T., Pfeifer, C., 2018. Optimization of nutrient and  
carbon recovery from anaerobic digestate via hydrothermal carbonization and  
investigation of the influence of the process parameters. *Waste Biomass Valor* 9,  
1303–1318. <https://doi.org/10.1007/s12649-017-9902-4>

Vardanyan, A., Kafa, N., Konstantinidis, V., Gu, S., Vyrides, I., 2018. Phosphorus  
dissolution from dewatered anaerobic sludge: Effect of pHs, microorganisms, and  
sequential extraction. *Bioresour. Technol. J.* 249, 464–472.  
<https://doi.org/10.1016/j.biortech.2017.09.188>

Villamil, J.A., Mohedano, A.F., Martín, J.S., Rodriguez, J.J., De la Rubia, M.A., 2020.  
Anaerobic co-digestion of the process water from waste activated sludge  
hydrothermally treated with primary sewage sludge. A new approach for sewage  
sludge management. *Renew. Energy* 146, 435–443.  
<https://doi.org/10.1016/j.renene.2019.06.138>

- Villamil, J.A., Mohedano, A.F., Rodriguez, J.J., De la Rubia, M.A., 2018. Valorisation of the liquid fraction from hydrothermal carbonisation of sewage sludge by anaerobic digestion. *J. Chem. Technol. Biotechnol.* 93, 450–456. <https://doi.org/10.1002/jctb.5375>
- Villamil, J.A., Mohedano, A.F., Rodriguez, J.J., De la Rubia, M.A., 2019. Anaerobic co-digestion of the aqueous phase from hydrothermally treated waste activated sludge with primary sewage sludge. A kinetic study. *J. Environ. Manage.* 231, 726–733. <https://doi.org/10.1016/j.jenvman.2018.10.031>
- Wang, L., Chang, Y., Liu, Q., 2019. Fate and distribution of nutrients and heavy metals during hydrothermal carbonization of sewage sludge with implication to land application. *J. Clean. Prod.* 225, 972–983. <https://doi.org/10.1016/j.jclepro.2019.03.347>
- Wang, Q., Li, J., Tang, P., Fang, L., Poon, C.S., 2018. Sustainable reclamation of phosphorus from incinerated sewage sludge ash as value-added struvite by chemical extraction, purification and crystallization. *J. Clean. Prod.* 181, 717–725. <https://doi.org/10.1016/j.jclepro.2018.01.254>
- Wang, T., Zhai, Y., Zhu, Y., Peng, C., Wang, Tengfei, Xu, B., Li, C., Zeng, G., 2017. Feedwater pH affects phosphorus transformation during hydrothermal carbonization of sewage sludge. *Bioresour. Technol.* 245, 182–187. <https://doi.org/10.1016/j.biortech.2017.08.114>
- Xu, Y., Yang, F., Zhang, L., Wang, X., Sun, Y., Liu, Q., Qian, G., 2018. Migration and transformation of phosphorus in municipal sludge by the hydrothermal treatment and its directional adjustment. *Waste Manag.* 81, 196–201. <https://doi.org/10.1016/j.wasman.2018.10.011>
- Yang, M., Xie, Q., Wang, X., Dong, H., Zhang, H., Li, C., 2019. Lowering ash slagging

and fouling tendency of high-alkali coal by hydrothermal pretreatment. *Int. J. Min. Sci. Technol.* 29, 521–525. <https://doi.org/10.1016/j.ijmst.2018.05.007>

Zhao, P., Shen, Y., Ge, S., Yoshikawa, K., 2014. Energy recycling from sewage sludge by producing solid biofuel with hydrothermal carbonization. *Energy Convers. Manag.* 78, 815–821. <https://doi.org/10.1016/j.enconman.2013.11.026>

Zhao, X., Becker, G.C., Faweya, N., Correa, C.R., Yang, S., Xie, X., 2018. Fertilizer and activated carbon production by hydrothermal carbonization of digestate. *Biomass Conv. Bioref.* 8, 423–436. <https://doi.org/10.1007/s13399-017-0291-5>